INHERENTLY DIGITAL MICRO CAPACITIVE TILT SENSOR FOR LOW POWER MOTION DETECTION

Li Zhao, Eric M. Yeatman
Optical and Semiconductor Devices Group, Department of Electrical and Electronic Engineering
Imperial College London, SW7 2AZ

Abstract: Low power body motion detection is useful for applications including long term monitoring and image registration for internal imaging. In this paper, a linearized inherently digital capacitive tilt sensor is presented, along with progress on MEMS fabrication. The device is designed for full range (–70° to +70°) tilt angle detection, and to generate linear digital output without analogue-to-digital conversion.

Keywords: inertial sensors, MEMS, electrostatic

I INTRODUCTION

Tilt sensors are important in motion detection systems, especially in medical science and health care applications, such as surgical tools, scan and restoration, gait studies and functional electrical stimulation [1]. Although high quality MEMS accelerometers are widely available, these are generally not optimized for tilt sensing, and have relatively high power consumption, mainly due to the signal conditioning circuits including A/D conversion. In self-powered wearable sensor networks, ultra low power tilt sensors could be integrated with other motion detectors and chemical sensors, e.g. glucose or pH sensors, in one highly compact package, to measure physical and biochemical changes simultaneously.

Tilt sensors using various sensing principles, such as piezoresistive and capacitive, are commonly used in motion detection systems. A capacitive type of sensor with the advantages of low temperature dependence, large dynamic range simple structure and low power consumption characteristics is described here. For typical capacitive sensors, the capacitance variation is caused by either changing the distance [2] or overlap area [3] between electrodes, or the permittivity of the dielectric material [4]. In our design, or the method of changing the overlap area is adopted, and a modified comb drive [5] structure is applied to maximise the output signals and lessen the power consumption by generating digital similar signals directly.

Previously, we have proposed an inherently digital tilt sensor with modified comb drive structures [6], which can generate periodic capacitive signals with respect to lateral displacement. In this paper, a linearized design is described, having an output which is periodically changing with respect to tilt angle. This tilt sensor has been fabricated on a SOI (silicon-on-isolator) wafer with double sided processing. A method similar to SCREAM (single crystal reactive etching and metallization) is applied to fully release the device from the substrate. Starting with a brief description of the device concept, the linearized structure is proposed with simulation results, and the fabrication is discussed in further detail.

II DEVICE CONCEPT AND STRUCTURE

The device is based on a monolithic proof mass on a flexure suspension. Upon tilting, gravity forces the proof mass toward one of the adjacent stationary comb electrodes; hence the capacitance increases at this side, while decreasing at the other. A 3D illustration of the device concept, as modeled in CoventorWare2006, is shown in Fig 1. The tilt angle can be detected by measuring the differential capacitance of the two electrodes through the interface circuits.

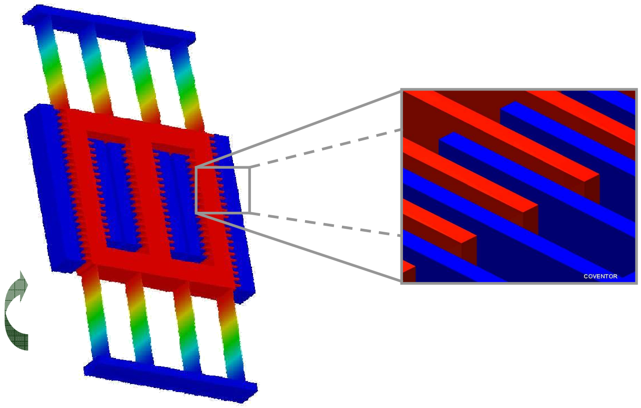

Figure 1. Operating principle of the tilt sensor and details of the comb drive structure.

An inherently digital sensor structure with groups of varying width finger electrodes has been proposed [6] based on the device concept and finger structure shown in Fig 1. Both the moving and fixed comb fingers have periodic protrusions, and when these come into alignment the capacitance is maximised. One possibility this allows is to directly implement a binary reader, with different periodicity of capacitance for each bit. The value of the bits can then be obtained by a simple binary comparator, either using differential electrodes or against a threshold value in the case of a single-sided device. In this structure, the capacitive output changes linearly with lateral displacement of the proof mass, which means the output is nonlinear with respect to the tilt angle. To solve this problem, a linearized modeled is developed and a 3 bit digital comb structure of this form (with only one finger pair per type shown for clarity) is illustrated in Fig 2. The space between protrusions is rearranged to compensate for the nonlinear relationship of the displacement and tilt angle. Fig 3 shows that the period of each bit is now uniform with respect to tilt angle. This simulation result is based on a 30 µm thick device and 500 finger pairs of each bit. A minimum separation of 1 µm between opposing protrusions is assumed.

An issue with this structure that is not negligible is the fringing field effect, which will tend to “blur” the variation. According to the modelling in [6], the optimised tooth-to-gap ratio to minimise the effect is 1/3. This limits the dynamic range of the sensor, because the space between protrusions is decreasing as the tilt angle increases. It is most severe in the least significant bit, as shown in Fig 3, because more protrusions are required to generate the periodic output. For a 100 µm long finger, tilt angles larger than 70° are hard to detect due to the fringing field effect. Longer fingers can be implemented; however, this will bring instability during the movement and difficulties in fabrication.

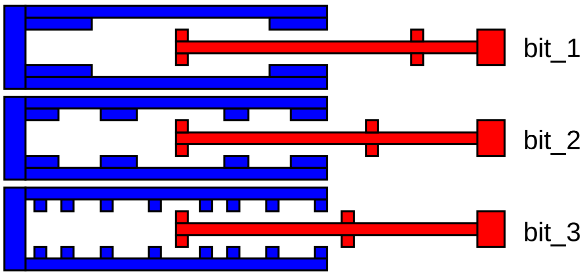

Figure 2. Schematic of the 3-bit digital comb drive.

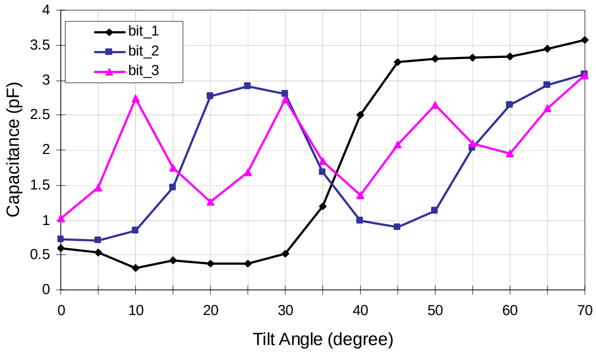

Figure 3. Output characteristic of the linearized digital tilt sensor.

A low power front-end circuit has been designed and fabricated by Constandinou [7]. The threshold value to distinguish “0” or “1” can be set between 2 pF and 2.5 pF. No A/D converter is required because of the periodic nature of the capacitance. This should greatly reduce the total power consumption of the sensing system.

III FABRICATION AND RESULTS

The tilt sensor is fabricated on a SOI wafer with the 50 µm silicon on the device layer, 500 µm silicon on the handle layer and 2 µm buried silicon dioxide in between. Two mask processing is applied. One is on the device layer to define the sensor structure, and the other is on the handle layer for back etching to release the proof mass. Since the device layer contained very fine patterns (comb fingers), which are difficult to protect from further processing, the fabrication started with the handle layer.

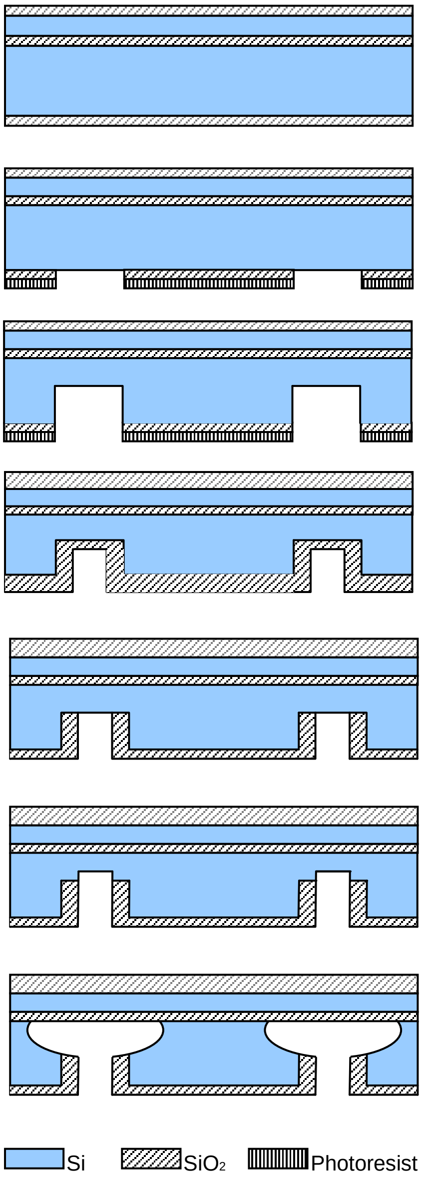

(a) Oxidation (48-hours, 1 µm)

(b) Pattern SiO_2 (mask)

(c) DRIE_1

(d) Oxidation (4-hour, 0.3 µm)

(e) Clear bottom silicon dioxide

(f) DRIE_2

(g) Isotropic release

Figure 4. Processing flow of handle layer

In order to fully release and isolate the movable part of the device and make the stationary part remain attached to the substrate, a method similar to SCREAM [8, 9] processing is conducted, as shown in Fig 4. First of all, a 48-hour oxidation is carried out to grow 1 µm silicon dioxide on both sides of the wafer [*Fig. 4 (a)*]. A thick layer of photoresist AZ9260 (10 μm) is applied to transfer the pattern from the handle layer mask onto the silicon dioxide [*Fig. 4 (b)*]. The patterned oxide acts as the mask for DRIE (deep reactive ion etching). The unmasked silicon is anisotropically etched 380 μm in depth [*Fig. 4 (c)*] to form cylindrical holes for later isotropic etching. Then the photoresist is stripped, and another oxide layer (0.3 μm) is deposited to cover the exposed side-wall of the etched trench [*Fig. 4 (d)*]. Anisotropic RIE (reactive ion etching) using CH_4 and Argon is carried out to remove the silicon dioxide at the bottom of the holes, while the oxide on the side wall remains. Since the oxide layer on the surface (48 hours of oxidation in total) is thicker than the oxide layer at the bottom (4 hours oxidation) of the holes, there is still oxide mask material left for further etching [*Fig. 4 (e)*]. Another DRIE step [*Fig. 4 (f)*] is needed to expose around 50 μm silicon on the side-wall to make the next isotropic etching more efficient. Finally, the device is ready to be released by isotropic etching, which only removes the silicon under the movable part and avoids dropping of the stationary islands [*Fig. 4 (g)*].

The processing flow of the device layer is shown in Fig. 5. The device layer contains very fine features which have the dimension of 2 μm. In this case, we have to use a very thin layer (<1 μm) of photoresist to transfer the device patterns onto the silicon. However, such thin photoresist is very critical as a mask for 50 μm DRIE. Therefore an extra layer of silicon dioxide is used as the etching mask on the device layer.

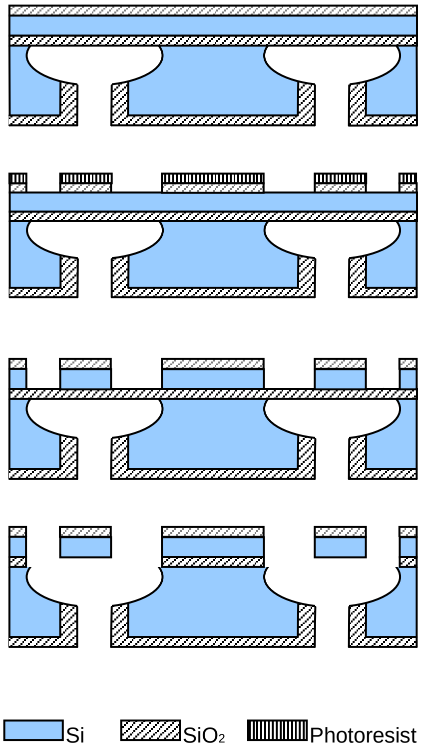

(a) Oxidation (14-hours, 0.5 μm*)*

(b) Pattern SiO_2 (mask)

(c) DRIE

(d) HF release

Figure 5. Processing flow of device layer

The silicon oxide grown from the handle layer processing is not suitable as a mask here, because patterning such thick oxide (~1.1 μm) requires thicker photoresist (>7 μm), which will also deteriorate the fine features. Therefore, before transferring the device pattern onto the wafer, we need to strip the previous oxide and grow a new layer of oxide for 14 hours (0.45 μm) [*Fig. 5 (a)*]. A thin layer of photoresist S1813 (1 μm) is applied to transfer the pattern onto the silicon dioxide mask [*Fig. 5 (b)*]. DRIE is then carried out to etch 40 μm [*Fig. 5 (c)*], continued with a low frequency etching to reduce the notching effect [10] when etching reaches the buried oxide layer. The whole device is fully released by HF etching to remove the buried oxide layer under the movable part.

We have overcome a number of difficulties in the fabrication progress. Fig 6 shows the micrographs from the scanning electron microscope (SEM).

First of all, fine features (1-2 μm) are very important for this sensor to get good performance. However, to transfer them to the silicon requires an extensive experimentation to find the best match of key parameters, including thickness of the photo-resist, soft baking time, UV exposure time and developing time. Low frequency processing is applied when etching approaches the oxide layer to reduce the notching effect, which is caused by the charge build up in the oxide. Fig 6 (a) shows the detailed structures with 2 μm finger width.

A very high aspect ratio of 25 is achieved by investigation of the optimized combination of gas flow and density, etching time and etching frequency with standard DRIE. Table 1 shows the process parameters on the device layer for the STS ICP Multiplex Etcher.

Table 1. Process for DRIE on device layer

	Etching	Passivation
Gas:	SF_6: 130 sccm	C_4F_8: 85 sccm
	O_2: 13 sccm	
Pressure:	22 mT	14 mT
Time:	7 sec / cycle	7sec / cycle

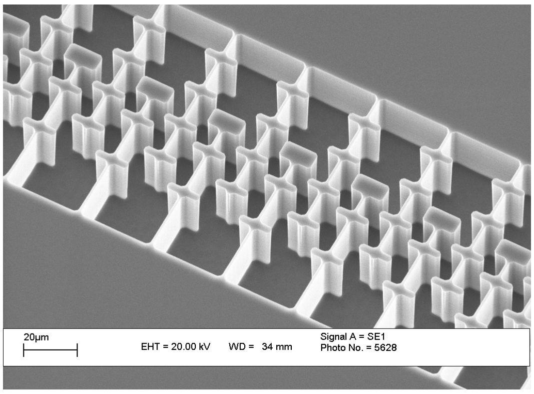

(a) the 2^{nd} bit of digital comb drive fingers

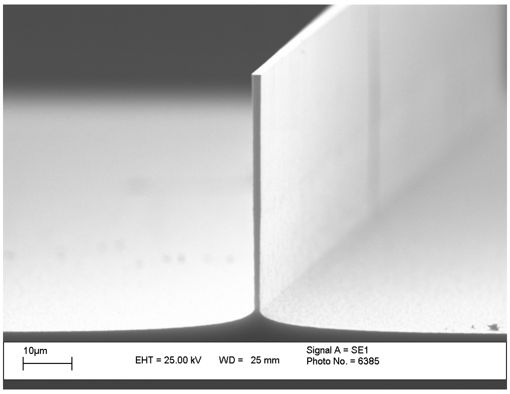

(b) Cross section of the suspension beam with high aspect ratio and high verticality

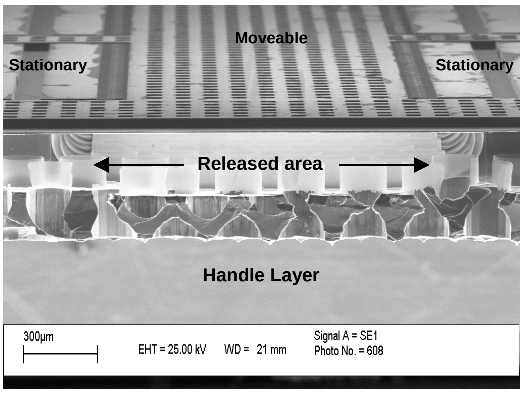

(c) Released movable mass by DRIE processing

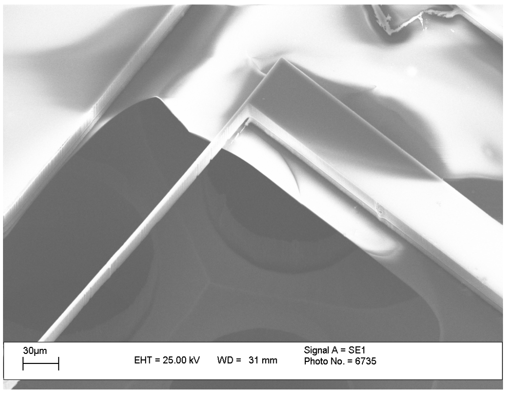

(d)released suspension beam

Figure 6. SEM micrographs of the tilt sensor.

The cross section of a suspension beam shown in Fig 6(b) has a width of 2 µm, depth of 50 µm and verticality of 89°. In Fig 6(c), the cross-section view of the movable mass released by handle layer processing is shown. Fig 6(d) shows one part of the released suspension beam. There is still some oxide remaining to be etched in HF.

IV CONCLUSIONS

A low power inherently digital tilt sensor generating linear capacitive output with respect to the tilt angle has been fabricated on silicon.

The resolution of the sensor can be increased by adding more bits on the mass. A tilt sensor with 5 bits could reach a resolution of ±1.5° for the least significant bit. As more bits are involved, the finger length and size of the devices will be increased. Moreover, it is getting more difficult to design and fabricate a more flexible beam structure without introducing much sag. However, this tilt sensor shows potential for systems driven by a limited power supply and not requiring very high resolution. One suitable application would be wearable Body sensor nodes. When other sensors, like heart pace detectors, are working, the information about the patient's movement, such as sleeping, walking or suddenly falling over, are extremely important.

A one mask process on each silicon layer has been applied, and optimized fabrication parameters based on the standard processing steps have been developed from extensive experiments. A fully functioning device remains to be demonstrated, and this is the subject of ongoing work.

REFERENCES

1. Dai, R., et al., *Application of tilt sensors in functional electrical stimulation.* Rehabilitation Engineering, IEEE Transactions on [see also IEEE Trans. on Neural Systems and Rehabilitation], 1996. 4(2): p. 63-72.
2. Kaienburg, J.R., Huonker, M., and Schellin, R., *Surface Micromachined Bridge Configurations for Accurate Angle Measurements*. in *Micro electro mechanical systems*. 2000. Miyazaki, Japan: IEEE.
3. Bantien, F., *Micromechanical Tilt Sensor*. 1992, Robert Bosch GmbH: United States.
4. Ueda, H., et al. *Micro Capacitive Inclination Sensor Utilizing Dielectric Nano-Particles*. in *IEEE, MEMS 2006*. 2006. Istanbul, Turkey.
5. Tang, W.C., et al., *Electrostatic-comb drive of lateral polysilicon resonators.* Sensors and Actuators A: Physical, 1990. 21(1-3): p. 328-331.
6. Zhao, L., Yeatman E.M., *Micro capacitive tilt sensor for human body movement detection.* Proc. Int. Workshop on Wearable and Implantable Body Sensor Networks, Aachen Germany, 2007.
7. Constandinou T.G., Georgiou J. and Toumazou, C., *Micropower front-end interface for differential-capacitive sensor systems.* IET Electronics Letters, 2008. Vol: 44.(No 7): p. pp. 470-472.
8. Shaw, K.A., Zhang, Z.L. and MacDonald, N.C., *SCREAM I: A single mask, single-crystal silicon, reactive ion etching process for microelectromechanical structures.* Sensors and Actuators A: Physical, 1994. 40(1): p. 63-70.
9. MacDonald, N.C., *SCREAM MicroElectroMechanical Systems.* Microelectronic Engineering, 1996. 32(1-4): p. 49-73.
10. Madou, M.J., *Fundamentals of Microfabrication: the science of miniaturization*. 2nd ed. 2002: CRC Press LLC. 723.